

Use of coherent control methods through scattering biological tissue to achieve functional imaging

Johanna M. Dela Cruz*, Igor Pastirk*, Matthew Comstock*, Vadim V. Lozovoy*, and Marcos Dantus*^{††}

Departments of *Chemistry and [†]Physics and Astronomy, Michigan State University, East Lansing, MI 48824

Communicated by James L. Dye, Michigan State University, East Lansing, MI, October 18, 2004 (received for review June 30, 2004)

We test whether coherent control methods based on ultrashort-pulse phase shaping can be applied when the laser light propagates through biological tissue. Our results demonstrate experimentally that the spectral-phase properties of shaped laser pulses optimized to achieve selective two-photon excitation survive as the laser pulses propagate through tissue. This observation is used to obtain functional images based on selective two-photon excitation of a pH-sensitive chromophore in a sample that is placed behind a slice of biological tissue. Our observation of coherent control through scattering tissue suggests possibilities in multiphoton-based imaging and photodynamic therapy.

pulse shaping | two-photon | femtosecond laser | intrapulse interference

Interest in coherent laser control has grown steadily, given its potential for influencing quantum-mechanical laser-molecule interactions (1–7). With the use of pulse shapers and computer learning algorithms, scientists have controlled the excitation of isolated atoms and molecules (8–10) and, more recently, large molecules in solution (11–13). Population transfer between different electronic states of large organic molecules can be maximized or minimized through manipulation of the spectral phase of ultrashort laser pulses (14, 15). The benefits of coherent laser control of large organic molecules can be extended to the biological field through selective two-photon chemical microenvironment probing (16) and microscopy (17). Control of laser-matter interactions could revolutionize biomedical applications. Coherent control schemes, for example, could enhance methods such as two-photon imaging (18, 19), which has provided higher resolution, lower background scattering, and better sample penetration than traditional techniques. Selective two-photon excitation would be desirable for distinguishing healthy from cancerous tissue based on differences in their chemical properties, such as pH, or for activating a photodynamic therapy (PDT) agent only when it is absorbed by cancer cells by using two-photon activated PDT (20). These improvements would be possible only if shaped laser pulses maintain their unique properties as they transmit through scattering biological tissue.

Coherent control of laser-induced processes is based on the quantum interference among multiple excitation pathways (3). Progress in this field has been fueled by advances in pulse-shaping technology, allowing control of the phase and amplitude across the bandwidth of ultrashort laser pulses (21). Control schemes depend on introducing intricate phase structures on the laser pulses that, by means of constructive and/or destructive interference, optimize the desired outcome and minimize other pathways. This dependence on the accurate phase structure of the pulse suggests that these methods may not be applicable to situations involving transmission through scattering biological tissue.

When a laser beam passes through a turbid scattering medium, its coherence (a property of waves defined as the degree with which waves are in step with each other) degrades exponentially as $I_{\text{coherent}} = I_0 \exp(-\mu_c x)$, where $1/\mu_c$ is the scattering length of the medium and x is the sample thickness. The transformations of the pulse and the exponential loss of coherence are shown

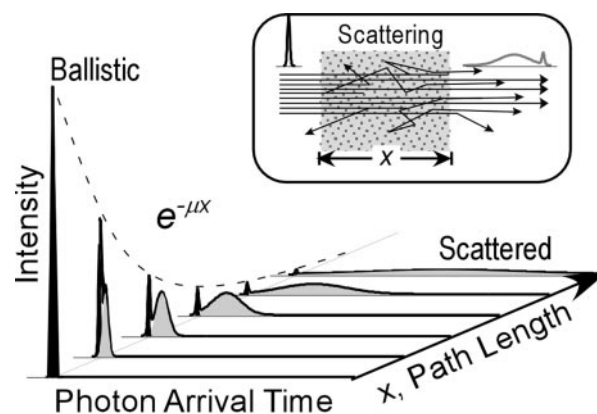


Fig. 1. Coherence degradation and pulse transformation as a function of scattering path length. As a short pulse of light enters a scattering medium, coherent, or ballistic, photons (narrow black peaks) are lost exponentially. The scattered photons (broad gray peaks), which lag in time, lose their coherence and are randomly delayed.

schematically in Fig. 1. The coherent component of the electric field, which is sometimes referred to as the ballistic photons (22), propagates through and maintains its directionality. The incoherent component, or diffusive photons (shaded broad region in Fig. 1), loses its directionality because of scattering and can no longer be used for high-resolution multiphoton imaging (23). In this context, one can also identify an intermediate component referred to as the snake photons, whose degree of coherence is still debated (24). Scattering of a laser in biological tissue results from the spatial variations of the sample caused by the different cellular structures and substructures with different indices of refraction, causing changes in the directionality of portions of the beam and introducing various delays.

In this article, we present experimental proof that coherent control of nonlinear optical processes based on phase-only shaping can be achieved in scattering biological tissue. For these experiments, we optimized selective two-photon excitation of a pH-sensitive probe molecule, 8-hydroxypyrene-1,3,6-trisulfonic acid (HPTS) using phase-shaped femtosecond pulses. Optimization of the laser-pulse phase structure was based on the spectroscopic changes exhibited by HPTS in acidic and alkaline environments. In Fig. 2, we show the chemical structure of HPTS. The hydroxylic proton has a pK_a of ≈ 7.5 and is promptly lost in response to an increase in the pH of its local environment. The absorption maximum of the protonated species changes from 400 to 450 nm upon deprotonation (Fig. 2). Interestingly, the fluorescence maximum is 515 nm in both acidic and alkaline

Freely available online through the PNAS open access option.

Abbreviations: BPS, binary phase shaping; HPTS, 8-hydroxypyrene-1,3,6-trisulfonic acid; MIIPS, multiphoton intrapulse-interference phase scan; PDT, photodynamic therapy; SHG, second harmonic generation; TL, transform-limited.

^{††}To whom correspondence should be addressed. E-mail: dantus@msu.edu.

© 2004 by The National Academy of Sciences of the USA

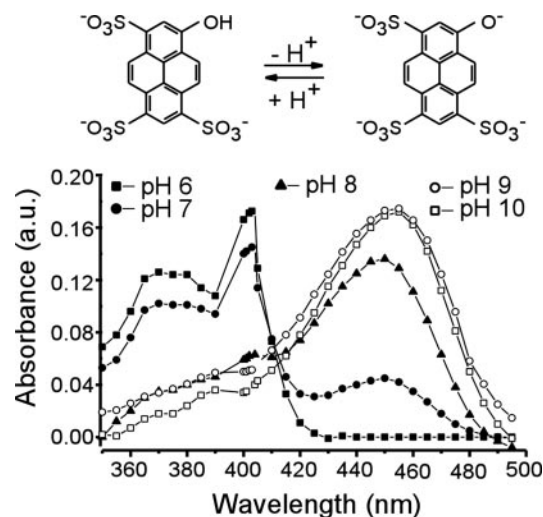


Fig. 2. Molecular formula and absorption spectra of HPTS in acidic and alkaline pH. Note that the loss of the hydroxylic proton leads to a large change in the absorption spectrum. a.u., arbitrary units.

pH, because the pK_a of the excited state molecule is much smaller, leading to fast deprotonation in all but highly acidic environments (25, 26). Laser-pulse optimization depends on the characteristics of the laser pulse (central wavelength, spectral phase, and pulse duration) and on multiphoton intrapulse interference (14–16), which leads to the suppression of two-photon excitation at certain wavelengths. We used an evolutionary learning algorithm (6) to obtain the greatest excitation selectivity between the two HPTS species (acidic and alkaline). This procedure was based on their known spectroscopy (see Fig. 2). We tested the selectivity achieved by two optimal phases during functional imaging with and without the presence of tissue. These phases, BPS06 and BPS10, maximize two-photon excitation of pH 6 or 10 solutions, respectively (26). Here, we present results that demonstrate selective two-photon excitation after a beam propagates through biological tissue. To better understand these results, we measured the rate of coherence loss with tissue depth, characterized the spectral phase of the pulses after they were transmitted through biological tissue, and characterized the signal intensity as a function of scattering and the resolution expected for possible biomedical applications of laser control.

Methods

The sample for the experiment is shown schematically in Fig. 3. It consists of three capillary tubes (i.d., 1 mm) filled with an acidic solution of HPTS placed in an alkaline solution of HPTS. Frozen raw chicken breast was sliced to a thickness of ≈ 1.5 –2.0 mm. The tissue was thawed and placed between the front face of the cell and a glass plate and slightly compressed to a uniform thickness of ≈ 0.5 mm. We found that the degree of compression did not affect the nonlinear optical signal. A drop of index-matching fluid was used between the tissue and the glass. We placed a transparent mask with printed letters “MSU” in front of the capillaries and behind the tissue as a reference.

The experiment was carried out by using a titanium–sapphire oscillator (Kapteyn–Murnane Labs, Boulder, CO) laser system. The laser spectrum was centered at ≈ 830 nm, with a bandwidth of 95 nm (full width at half maximum), corresponding to a 10-fs pulse duration. The large bandwidth is desirable to overlap the absorption of the two HPTS species (see Fig. 2) by two-photon excitation with the single pulse. The laser was sent to a prism-pair compressor and a broad-bandwidth pulse shaper (21). At the

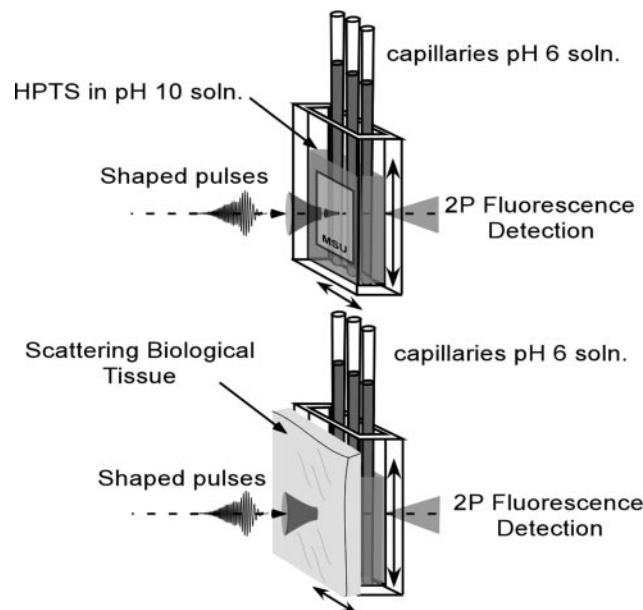


Fig. 3. Experimental setup used for selective two-photon (2P) excitation through scattering tissue. The sample consists of three 1-mm capillaries containing an acidic solution (soln.) of HPTS submerged in a quartz cell filled with an alkaline solution of HPTS. The sample was raster scanned (without and with scattering tissue) in the focal plane of the beam during data acquisition to obtain the images.

pulse shaper, the pulse is spectrally dispersed by a prism and collimated by a cylindrical mirror in an arrangement that is similar to a spectrometer. A computer-controlled spatial light modulator located at this position controls the phase and amplitude of the frequency components of the pulse. Subsequently, a second prism-mirror arrangement reconstitutes the pulse. A more detailed discussion on pulse shaping is given in ref. 21. A more detailed description of our pulse shaper is given in refs. 16 and 27.

The laser pulses were calibrated and compensated to transform-limited (TL) pulses at the position of the sample after a microscope objective by using the multiphoton intrapulse-interference phase scan (MIIPS) method (16, 27). This step is critical because it removes unwanted phase deformation introduced by the objective and other optics in the path of the laser beam. Starting from TL pulses, the condition in which all frequency components are in step with each other with a zero phase difference (a blank canvas), ensures reproducible results. The optimized spectral phase functions used for this experiment are based on binary phase shaping (BPS) (28), a method that assigns phase values of either zero or π to frequency components of the pulse instead of allowing arbitrary phase and amplitude values and is ideally suited for controlling multiphoton transitions. By restricting all of the possible values to just two, the search parameter space for the optimum pulses is reduced by >100 orders of magnitude (28), ensuring a more thorough search by the genetic algorithm.

Images were obtained by raster scanning the sample at the focal plane of the laser with and without scattering tissue. The laser was focused on the capillaries by a $\times 20$ objective (0.45 numerical aperture, Plan Fluor extended long working distance, Nikon); see Fig. 3. The energy per pulse entering the objective was 1 nJ. The resulting fluorescence from the sample was filtered by using a broadband filter (BG40) and a spectrometer with the detection wavelength set at 515 nm (resolution, 24 nm) and averaged point by point using a lock-in amplifier to obtain the two-dimensional (6×8 mm) image. Submicrometer resolution

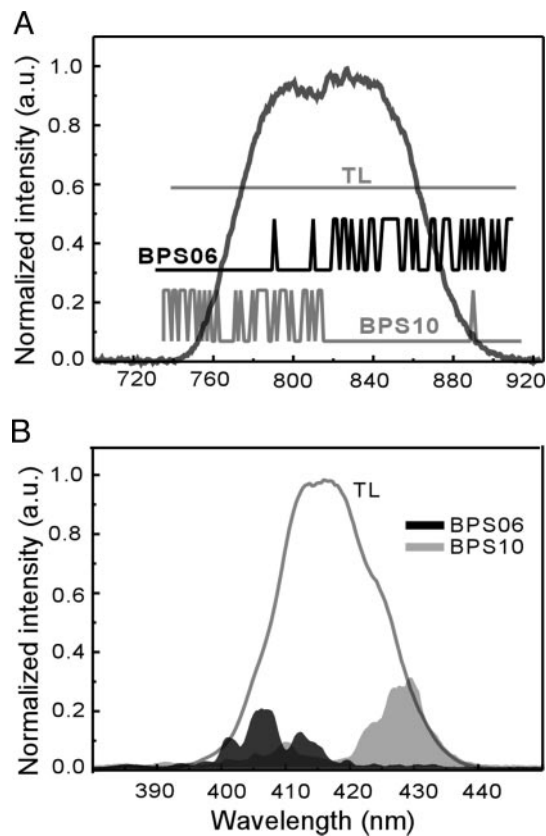


Fig. 4. Spectroscopic characterization of the laser pulses and the spectral phases used to control their nonlinear excitation properties. (A) Experimental spectrum of the femtosecond laser pulses centered near 830 nm. Three different phase functions were used in the experiment: TL pulses with a flat spectral phase and shaped pulses optimized for excitation of HPTS in acidic and alkaline environments, BPS06 and BPS10, respectively. (B) Experimental SHG spectra obtained from TL pulses and SHG spectra obtained when the phase functions BPS06 and BPS10 were introduced by the pulse shaper. Note that BPS06 suppresses SHG at longer wavelengths, and BPS10 suppresses SHG generation at shorter wavelengths. a.u., arbitrary units.

could be achieved by this method; however, the goal here is mainly to demonstrate that selective excitation is maintained through scattering tissue.

Results and Discussion

Functional Imaging. Imaging of the capillary tubes requires laser pulses that selectively excite HPTS in acidic or alkaline solution. Nonselective excitation, as would be obtained from TL pulses, cannot distinguish between the two solutions because HPTS in both environments has an approximately equal integrated cross-section of excitation and fluoresces at 515 nm. In Fig. 4, we show the spectral phase for TL pulses (a flat line) and the binary phase functions that were used to enhance excitation of HPTS in an acidic or an alkaline environment. The second harmonic generation (SHG) spectrum obtained from a thin nonlinear optical crystal (Fig. 4B) provided a diagnostic test of the effects of phase modulation. SHG has the same square dependence on the intensity of the laser pulses as two-photon excitation. Unlike the TL pulses, the shaped pulses preferentially excite one of the two different pH solutions. The complicated binary phase introduced in each of the shaped pulses involves several frequencies at which the phase of the light is retarded by π , which is equivalent to 1.3 fs. These seemingly small variations lead to the observed changes in the SHG spectrum. However, the spectrum of the laser pulse does not change upon phase modulation; only

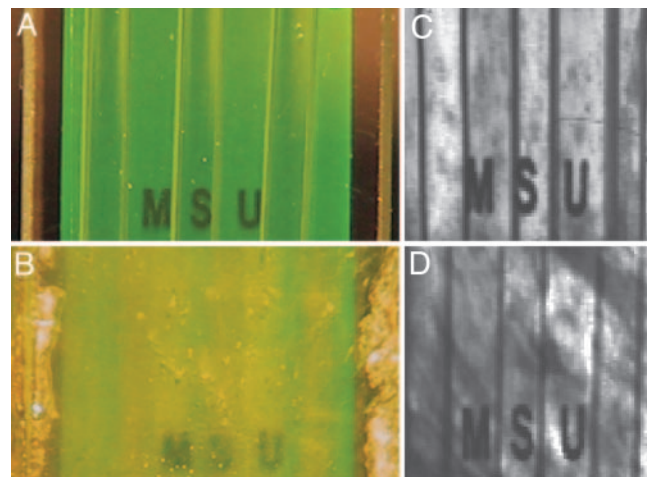


Fig. 5. Experimental sample with and without biological tissue imaged by a conventional camera and by two-photon imaging. (A and B) Photographs of the sample obtained under white-light illumination in the absence and presence of biological tissue. In both of these photographs, the three capillaries in the sample are difficult to distinguish. (C and D) Two-photon excitation images obtained by raster scanning the sample without and with scattering tissue, respectively. The walls of the capillary tubes, which appear as vertical lines, are $\approx 300 \mu\text{m}$ thick and are clearly visible in both images. Note that comparable image quality is obtained in the presence and absence of biological tissue. C and D were obtained with TL pulses, which are not capable of discriminating between the two different pH solutions.

its potential to cause two-photon excitation or generate second harmonic radiation at specific wavelengths is changed (14, 15).

Photographs of the sample are shown in Fig. 5A and B without and with biological tissue, respectively. The capillaries containing HPTS in acidic buffer are barely distinguishable from the alkaline HPTS solution in which they are immersed. Two-photon images obtained with TL pulses without and with biological tissue are displayed in Fig. 5C and D, respectively. The walls of the capillary tubes ($\approx 300 \mu\text{m}$) appear black because fluorescent solution is excluded by the wall. This observation confirms the confocal effect gained by two-photon excitation (18, 19). Note that we get a comparable quality of imaging with and without tissue.

The full effect of coherent control when using BPS is shown in Fig. 6. The image obtained with phase BPS06 enhances the signal from the capillaries (Fig. 6A), whereas the image obtained with phase BPS10 enhances the signal from the surrounding solution (Fig. 6B). By dividing the data from Fig. 6A by the data from Fig. 6B, we obtained the functional image shown in Fig. 6C. The image in Fig. 6D corresponds to the functional image obtained in the presence of biological tissue. The very high contrast between the three capillaries containing acidic solution and the surrounding alkaline solution is accentuated by false coloring in the top half of the images (Fig. 6C and D). The contrast between the two solutions is very clear even when the laser has transmitted through the tissue.

Loss of Coherence as a Function of Scattering. The striking functional images shown in Fig. 6 raise questions regarding the propagation of shaped and unshaped pulses through scattering media. Here, we describe experiments that are aimed at establishing the general physics responsible for the observation and at estimating the limits to future applications.

First, we measured the loss of ballistic photons as a function of scattering. For this experiment, the microscope objective focused the beam onto a $25\text{-}\mu\text{m}$ -diameter pinhole after transmission through a variable scattering medium consisting of a solution of skim milk in water in a 1-cm path-length cell. A 20%

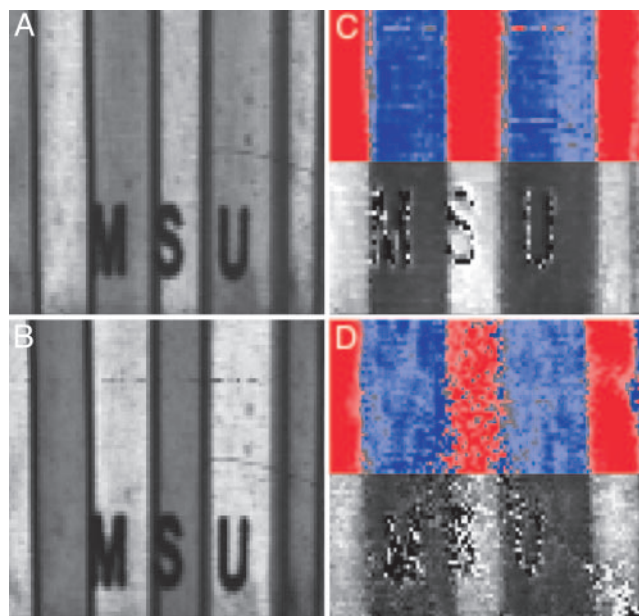


Fig. 6. Coherent control was used here to obtain pH-sensitive functional imaging. (A and B) Images obtained by two-photon excitation using the optimized phases BPS06 and BPS10, respectively. Note that the signal from the 1-mm capillary tubes is enhanced for BPS06 (A) and suppressed for BPS10 (B). (C) A functional image highlighting the contrast possible by using coherent control. This image was obtained by taking the ratio of the data obtained by BPS06/BPS10. (D) The functional image obtained when a slice of biological tissue was placed in front of the sample. Note that the presence of the tissue reduces the overall signal-to-noise ratio, but the discrimination between acidic and alkaline HPTS is conserved. The contrast in the functional images can be further enhanced by using false color (C Upper and D Upper). Higher values are shown in red, and lower values are shown in blue.

increase in the concentration of milk decreased the intensity of the transmitted light by 1 order of magnitude. The light emerging from the pinhole was measured by using a photomultiplier and a lock-in amplifier. We compared the loss of unscattered photons from TL pulses and shaped pulses. For this experiment, we used a phase mask that did not favor two-photon excitation at a particular wavelength to demonstrate that there is nothing unique about the rate of coherence loss for shaped or unshaped pulses. The results from these measurements are plotted in Fig. 7. The scattering of photons from both TL (filled squares) and phase-shaped (filled circles) pulses was found to increase exponentially as the percentage of skim milk in the solution was increased.

Phase shaping does not affect the rate of decoherence, which is caused by the spatial inhomogeneities in the scattering medium. The loss of photons arises from their random collision with particles in the scattering medium, and phase shaping does not alter the scattering probability. Because the scattering of photons is caused by spatial inhomogeneities in the sample, it cannot be corrected or prevented by spectral phase shaping.

By replacing the pinhole with an SHG crystal (20 μm $\beta\text{-BaB}_2\text{O}_4$ type I crystal), we confirmed that only the ballistic photons participate in generating second harmonic light (29). The SHG spectra of the TL and shaped pulses are shown in Fig. 7 Lower Inset. Note that the shaped pulses generate a weak, evenly distributed spectrum. The intensity dependence of the integrated second harmonic light from TL and shaped pulses was found to decay exponentially with a slope that is a factor of 2 greater than that obtained for the fundamental wavelength. This result is consistent with the expected dependence for two-photon response of $I_{\text{SHG}} = I_0 \exp(-2\mu_c x)$. These measurements, which

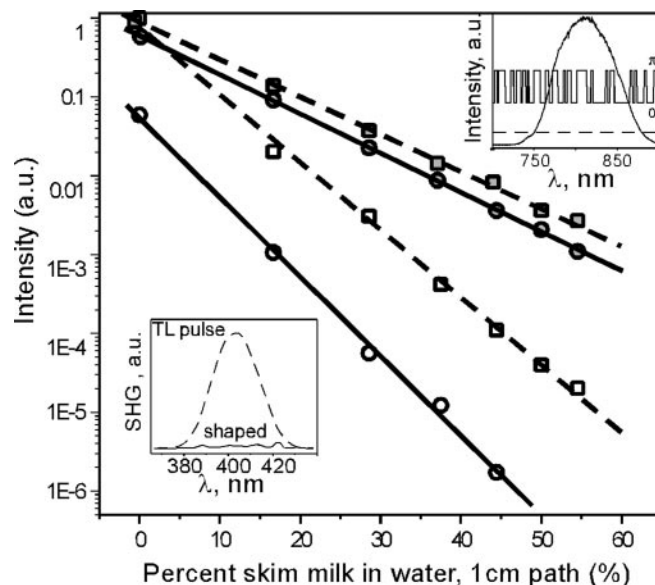


Fig. 7. Loss of coherent photons as a function of scattering. The transmitted ballistic photons from TL (squares) and shaped (circles) pulses were measured as a function of scattering. The phase shape for these measurements was chosen to suppress SHG generation evenly through the entire spectrum (see text). The intensity of the ballistic photons measured at 800 nm (filled symbols) was found to decay exponentially for both TL and shaped pulses. The intensity of the coherent photons was measured after SHG in a thin SHG crystal (open symbols). Greater scattering by a factor of 2 was recorded in this case, given the square dependence of SHG, confirming that only ballistic photons generate the second harmonic light. The spectrum and phase for the TL and shaped pulses used in this measurement are shown in Upper Inset. The spectrum of the SHG output from TL and shaped pulses are shown in Lower Inset. Note that the spectra of TL and shaped pulses are virtually identical (Upper Inset), but the phase structure of the shaped pulses decreases their ability to generate second harmonic light (Lower Inset). We find the same slope for both TL and shaped pulses; hence, they experience the same rate of scattering. a.u., arbitrary units.

range over more than 5 orders of magnitude in intensity, establish that only the ballistic photons are coherent and are responsible for SHG, that they are lost exponentially, and that spectral phase shaping does not affect this fundamental property. The data in Fig. 7 show that it is possible to transmit ballistic photons with spectral phase information to depths at which SHG intensity has dropped by 6 orders of magnitude. Additional efforts in noise suppression would allow us to go even deeper, or to collect back-scattered signal.

In Fig. 8, we show the SHG spectrum generated with TL pulses and the spectrum generated by using BPS10 shaped pulses without a scattering medium and with a solution of 15% of skim milk in water in a 1-cm path length cell. Note that the second harmonic spectrum of the shaped pulses is unaffected (except in overall intensity) by scattering. There is a slight change that arises from the wavelength dependence of Rayleigh scattering after four scattering lengths, which results in a slight attenuation at shorter (≈ 750 nm) compared with longer (≈ 850 nm) wavelengths. We confirm that phase shaping does not lead to a loss of optical resolution. Fig. 8 Inset, shows the image of 15 μm in diameter FluoSpheres (450/480, Molecular Probes). The fluorescent probes were deposited on a microscope slide and then covered by a 1-mm-thick slice of biological tissue and covered by a second microscope slide. The sample was raster scanned in front of the laser, which impinged first on the tissue and then on the spheres. The image, obtained by using BPS10, showed no loss of resolution when compared with that obtained by using TL pulses (data not shown).

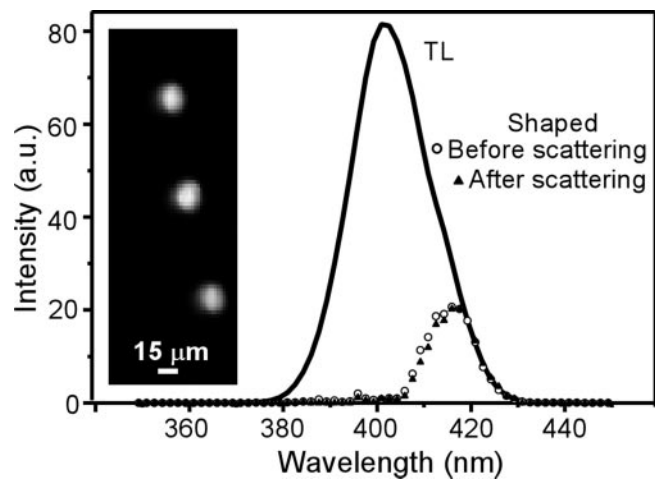


Fig. 8. SHG spectra generated for TL pulses and shaped pulses optimized for pH 10 without a scattering medium and after propagating through a 15% skim milk-in-water solution (equivalent to 2.1 scattering lengths). The spectrum after scattering was normalized to the intensity of the unscattered spectrum. We found that scattering does not change the observed SHG spectrum except for the overall intensity. (Inset) Three FluoSpheres of 15- μm diameter behind a 1-mm-thick slice of biological tissue. This image demonstrates that high resolution (μm) can be achieved by the shaped pulses after they transmit through biological tissue. a.u., arbitrary units.

The coherent control method presented for functional imaging is less expensive and simpler to carry out than current methods of multiphoton imaging. The pulse shaper compensates the pulses automatically by using MIIPS and introduces the optimum phases required for selective excitation. This method should be contrasted to an effort in which two expensive 100-fs pulsed lasers tuned to 800 and 900 nm and aligned to focus at the exact same spot would be used to reproduce the observed results. Alternatively, the use of an expensive tunable 100-fs laser would require tuning, alignment, and compression after the objective, which are procedures that are typically time-consuming and require a certain degree of expertise. Therefore, the ultrashort laser oscillator with a pulse shaper provides a more powerful and flexible platform.

We have measured directly the spectral phase of the laser pulses after transmission through biological tissue (1-mm chicken breast compressed to ≈ 0.25 mm). For these experiments, we used the MIIPS method (16, 26) and compared the spectral phase obtained when the laser transmitted through the tissue to the phase obtained through a similar thickness of glass. The MIIPS traces without and with biological tissue are shown in Fig. 9 *Upper* and *Lower Insets*, respectively. The retrieved spectral phases, shown in Fig. 9, show very small distortions (< 0.1 rad) in the 820- to 870-nm spectral region. More significant spectral phase distortion is observed for shorter wavelengths (790–820 nm). Note that the small distortion does not affect the desired selective excitation. If the distortion is more significant, it can be measured and compensated by MIIPS.

Conclusions

The successful use of coherent control to demonstrate functional imaging through a scattering medium (Fig. 6) leads us to expect that selective two-photon excitation and imaging could be achieved at greater depths of tissue (3–4 mm) (29, 30) by using coherent control. We have confirmed our ability to measure two-photon fluorescence through 4 mm of chicken breast tissue by using amplified laser pulses (unpublished work). For medical applications, endoscopes can be used to deliver the laser pulses to some of the internal organs, allowing therapeutic treatment of internal organs. The maximum amount of laser light that can be used on living tissue is regulated by safety concerns (American

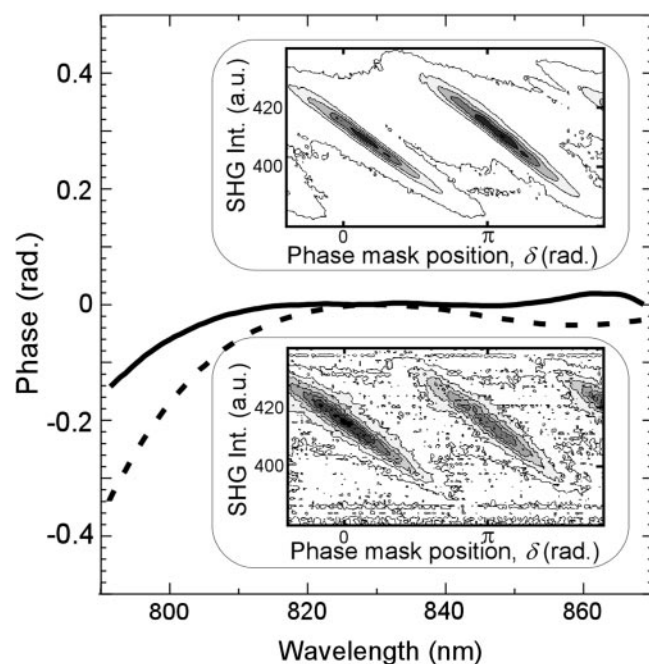


Fig. 9. Characterization of spectral phase of the laser pulses by using the MIIPS method without (solid line) and with (dashed line) biological tissue. The raw data are shown in *Insets*. Note that the presence of the tissue reduces the overall signal-to-noise ratio in the bottom MIIPS trace. Phase distortion is minimal for the longer wavelengths (820–870 nm). For shorter wavelengths, phase distortion is more significant. However, even at 790 nm, the 0.2-rad distortion is 1 order of magnitude smaller than the value of π used for the BPS functions, which is why binary phase functions successfully achieved the selective two-photon excitation that is required for functional imaging. Int., intensity; a.u., arbitrary units.

National Standards Institute Z163.1) and ultimately limits the maximum depth that could be achieved by the method described here. Three-photon-induced laser damage, which could result from the use of intense ultrashort pulses (31, 32), can be suppressed by orders of magnitude by using BPS, while preserving the large two-photon excitation yield obtained by these pulses. This suppression results from lengthening of the pulse due to the phase structure and from the destructive interference for three-photon excitation pathways (15).

The purpose of our experiment was to determine whether coherent control methods based on spectral phase modulation and multiphoton intrapulse interference could be used under typical scattering conditions encountered in biological imaging to provide discrimination for laser-based imaging or therapeutic purposes. Given that we found an affirmative answer to this question, possibilities afforded by coherent control could be exploited. In the experiment presented here, functional imaging (as shown here with pH, but also possible with Ca^{2+} , Na^+ , biomarkers, and drug gradients) was demonstrated by optimizing the spectral phase of the laser pulses by using a pulse shaper, without laser tuning or fluorescence filters. These advances could enhance noninvasive two-photon imaging methods (33, 34) by providing contrast mechanisms based on selective-probe excitation while minimizing the risk of damaging healthy tissue. Our findings should inspire new possibilities for the use of shaped pulse lasers in the biomedical field.

We thank Profs. Kenneth Eisenthal and James K. McCusker for valuable feedback on the manuscript. This work was supported by the Chemical Sciences, Geosciences, and Biosciences Division of the U.S. Department of Energy Office of Basic Energy Sciences. M.D. is a Camille Dreyfus Teacher-Scholar.

1. Judson, R. S. & Rabitz, H. (1992) *Phys. Rev. Lett.* **68**, 1500–1503.
2. Zare, R. N. (1998) *Science* **279**, 1875–1879.
3. Gordon, R. J. & Rice, S. A. (1997) *Annu. Rev. Phys. Chem.* **48**, 601–641.
4. Rice, S. A. (2001) *Nature* **409**, 422–426.
5. Rice, S. A. & Shah, S. P. (2002) *Phys. Chem. Chem. Phys.* **4**, 1683–1700.
6. Rabitz, H. (2003) *Science* **299**, 525–527.
7. Dantus, M. & Lozovoy, V. V. (2004) *Chem. Rev.* **104**, 1813–1860.
8. Assion, A., Baumert, T., Bergt, M., Brixner, T., Kiefer, B., Seyfried, V., Strehle, M. & Gerber, G. (1998) *Science* **282**, 919–922.
9. Levis, R. J., Menkir, G. M. & Rabitz, H. (2001) *Science* **292**, 709–713.
10. Weinacht, T. C. & Bucksbaum, P. H. (2002) *J. Opt. B* **4**, R35–R52.
11. Bardeen, C. J., Yakovlev, V. V., Wilson, K. R., Carpenter, S. D., Weber, P. M. & Warren, W. S. (1997) *Chem. Phys. Lett.* **280**, 151–158.
12. Brixner, T., Damrauer, N. H., Niklaus, P. & Gerber, G. (2001) *Nature* **414**, 57–60.
13. Herek, J. L., Wohlleben, W., Cogdell, R. J., Zeidler, D. & Motzkus, M. (2002) *Nature* **417**, 533–535.
14. Walowicz, K. A., Pastirk, I., Lozovoy, V. V. & Dantus, M. (2002) *J. Phys. Chem. A* **106**, 9369–9373.
15. Lozovoy, V. V., Pastirk, I., Walowicz, K. A. & Dantus, M. (2003) *J. Chem. Phys.* **118**, 3187–3196.
16. Dela Cruz, J. M., Pastirk, I., Lozovoy, V. V., Walowicz, K. A. & Dantus, M. (2004) *J. Phys. Chem. A* **108**, 53–58.
17. Pastirk, I., Dela Cruz, J. M., Walowicz, K. A., Lozovoy, V. V. & Dantus, M. (2003) *Opt. Express* **11**, 1695–1701.
18. Denk, W., Strickler, J. H. & Webb, W. W. (1990) *Science* **248**, 73–76.
19. Denk, W. (1996) *J. Biomed. Opt.* **1**, 296–304.
20. Fisher, W. G., Partridge, W. P., Dees, C. & Wachter, E. A. (1997) *Photochem. Photobiol.* **66**, 141–155.
21. Weiner, A. M. (2000) *Rev. Sci. Instrum.* **71**, 1929–1960.
22. Yoo, K. M. & Alfano, R. R. (1990) *Opt. Lett.* **15**, 320–322.
23. Hee, M. R., Izatt, J. A., Jacobson, J. M., Fujimoto, J. G. & Swanson, E. A. (1993) *Opt. Lett.* **18**, 950–952.
24. Parys, B., Allard, J. F., Desmullier, F., Houde, D. & Cornet, A. (2004) *J. Opt. A* **6**, L23–L27.
25. Tran-Thi, T. H., Gustavson, T., Prayer, C., Pommeret, S. & Hynes, J. T. (2000) *Chem. Phys. Lett.* **329**, 421–430.
26. Tran-Thi, T. H., Prayer, C., Millie, P. H., Uznanski, P. & Hynes, J. T. (2002) *J. Phys. Chem. A* **106**, 2244–2255.
27. Lozovoy, V. V., Pastirk, I. & Dantus, M. (2004) *Opt. Lett.* **7**, 775–777.
28. Comstock, M., Lozovoy, V. V., Pastirk, I. & Dantus, M. (2004) *Opt. Express* **12**, 1061–1066.
29. Beaurepaire, E., Oheim, M. & Mertz, J. (2001) *Opt. Commun.* **188**, 25–29.
30. Theer, P., Hasan, M. T. & Denk, W. (2003) *Opt. Lett.* **28**, 1022–1024.
31. Koester, H. J., Baur, D., Uhl, R. & Hell, S. W. (1999) *Biophys. J.* **77**, 2226–2236.
32. Hopt, A. & Neher, E. (2001) *Biophys. J.* **80**, 2029–2036.
33. Szmajcinski, H., Gryczynski, I. & Lakowicz, J. R. (1998) *Biospectr.* **4**, 303–310.
34. Konig, K. (2000) *J. Microsc. (Oxford)* **200**, 83–104.